



HAL
open science

Revealing the Friction Stress of Microalgae in Microfluidic Devices through Mechanofluorochromism

Lorenzo Casimiro, Rémi Métivier, Bruno Le Pioufle, Sakina Bensalem,
Clémence Allain

► **To cite this version:**

Lorenzo Casimiro, Rémi Métivier, Bruno Le Pioufle, Sakina Bensalem, Clémence Allain. Revealing the Friction Stress of Microalgae in Microfluidic Devices through Mechanofluorochromism. *Advanced Materials Interfaces*, 2023, 10.1002/admi.202300312 . hal-04190604

HAL Id: hal-04190604

<https://hal.science/hal-04190604>

Submitted on 29 Aug 2023

HAL is a multi-disciplinary open access archive for the deposit and dissemination of scientific research documents, whether they are published or not. The documents may come from teaching and research institutions in France or abroad, or from public or private research centers.

L'archive ouverte pluridisciplinaire **HAL**, est destinée au dépôt et à la diffusion de documents scientifiques de niveau recherche, publiés ou non, émanant des établissements d'enseignement et de recherche français ou étrangers, des laboratoires publics ou privés.



Distributed under a Creative Commons Attribution - NonCommercial - NoDerivatives 4.0 International License

Revealing the Friction Stress of Microalgae in Microfluidic Devices through Mechanofluorochromism

Lorenzo Casimiro, Rémi Métivier, Bruno Le Pioufle, Sakina Bensalem,* and Clémence Allain*

Polydiacetylenes are deeply investigated for their mechanofluorochromic behavior: the blue, non-emitting solid phase, obtained by photopolymerization of the diacetylene precursor, is converted to the red, emitting one by a mechanical stimulus. Inspired by the great potentiality of these compounds to act as microscale force probes, the mechanofluorochromism is implemented in microalgae biotechnology. Indeed, mechanical solicitations in a microfluidic chip can weaken the cellular envelope and facilitate the extraction of high-added value compounds produced by the microalgae. Herewith, a polydiacetylene-based mechanofluorochromic sensor is reported to be able to detect the stress applied to microalgae in microchannels. A triethoxysilane diacetylene precursor is designed that photopolymerizes in a purple, low-emissive phase, and is converted to the red, high-emissive phase upon mechanical stress. Hereafter, a protocol is set up to chemically graft in the microfluidic channels a polydiacetylene layer, and eventually proves that upon compression of *Chlamydomonas reinhardtii* microalgae in restricted areas, the friction stress is revealed by the mechanofluorochromic response of the polydiacetylene, leading to a marked fluorescence enhancement up to 83%. This prototype of microscale force probes lays the ground for microscale stress detection in microfluidics environments, which can be applied not only to microalgae but also to any mechano-responsive cellular sample.

yield high-value fuels. As such, microalgae are nowadays considered as one of the most valuable tools to address the utmost urgent issue of energy demand.^[4–16] In this framework, our group has recently focused on the possibility to mechanically weaken the cellular envelope of microalgae with a microfluidic device specifically designed to compress the cells in a series of channels containing restricted areas.^[17–19] Despite we successfully proved that the mechanical compression weakens the cellular envelope of *Chlamydomonas reinhardtii* microalgae,^[17] further quantification of these mechanical solicitations remains necessary in order to successfully upscale our protocol. Thus, our protocol requires a smart force sensor, able to probe the microscale stress applied to the cells and localize it within the confined environment of the device, ideally with simple and non-destructive detection methods.

A powerful molecular bottom-up approach to address this issue is provided by mechanofluorochromism,^[20–24] i.e., the ability of some solid materials

or molecular assemblies – such as polymers, crystals, single molecules, monolayers, vesicles, or dyes dispersed in polymeric matrixes – to change their emission properties upon the application of a mechanical input. The mechanisms behind such an optical feature rely on the mechanically induced structural rearrangement of the material, which can cause a transition to a new polymeric^[25–28] or crystalline phase.^[29–31]


Among the several classes of mechanofluorochromes, a prominent position is covered by polydiacetylenes (PDAs),^[23,32–39] whose optical properties have been widely investigated (see reports from Schott,^[40] Filhol,^[41] and Carpick^[33,42]). These polymeric materials are formed by topotactic polymerization – via UV light, gamma rays irradiation, or heating – of colourless diacetylene precursors. The reaction can be easily achieved not only in the solid phase, but also in different polymer matrices,^[43] in monolayers,^[44–46] vapor deposited films,^[47] or vesicles.^[34,48] Polymerization usually yields PDA in the metastable “blue” phase, which absorbs with a structured band centered at 640 nm,^[33,36,40,47,49] hence the name, and does not show any detectable fluorescence. A second transition occurs upon temperature increase,^[44] chemical^[46] or

1. Introduction

Microalgae have raised great interest in biotechnology for their ability to accumulate in their cytoplasm large amounts of lipids,^[1–3] which can be extracted and further processed to

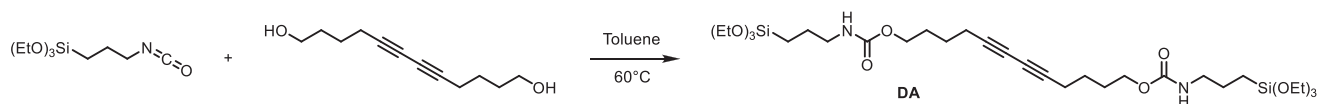
L. Casimiro, R. Métivier, C. Allain
 Université Paris-Saclay
 ENS Paris-Saclay, CNRS, PPSM, Gif-sur-Yvette 91190, France
 E-mail: clemence.allain@ens-paris-saclay.fr

B. Le Pioufle, S. Bensalem
 Université Paris-Saclay
 ENS Paris-Saclay, CNRS, Institut d'Alembert, LuMIn,
 Gif-sur-Yvette 91190, France
 E-mail: sakina.bensalem@ens-paris-saclay.fr

 The ORCID identification number(s) for the author(s) of this article can be found under <https://doi.org/10.1002/admi.202300312>

© 2023 The Authors. Advanced Materials Interfaces published by Wiley-VCH GmbH. This is an open access article under the terms of the Creative Commons Attribution License, which permits use, distribution and reproduction in any medium, provided the original work is properly cited.

DOI: 10.1002/admi.202300312



Scheme 1. Reaction scheme for the synthesis of the precursor DA.

biochemical interaction,^[50] solvent fuming,^[48] or mechanical stimulus,^[28,42,51–53] and consists in a molecular and supramolecular rearrangement in a “red” phase, which absorbs at 550 nm and usually emits ≈ 650 nm.^[32–34,40,42,47] The mechanism behind this phase transformation is still under investigation and debate, but it is most commonly reputed to depend on a partial loss in the conjugation of the alternated double and triple bonds and to a rearrangement of the side chains that releases the tension accumulated during the photopolymerization.^[28,33,40] As a result, the absorption is shifted toward higher energies, and the color changes accordingly. It must be underlined that red PDA cannot be considered as a simple polymorph of the blue one, but rather a different phase.^[40,41] The blue-to-red transition is usually irreversible;^[42] however, it can be preceded by a reversible transition from the blue phase to a metastable purple phase, characterized by a broad absorption band ≈ 600 nm partially overlapped to the blue and red phase spectra, which eventually transforms irreversibly into the red one. Several studies^[33,41,45,54,55] based on the kinetics and on the partial reversibility of these transitions have highlighted that the purple phase is indeed a different phase of PDA, rather than a mixture of blue and red PDA forms. Nevertheless, the optical properties are strongly dependent on the nature and spatial arrangement of the side groups of the polydiacetylene chain, as well as on the chemical environment and the applied stimuli. The versatility and the colorimetric and fluorometric response of PDA-based materials have stimulated the ingenuity of chemists for their wide field of possible applications, for example as sensors for ions, pH, or temperature,^[32,37,50,53,56–59] as biosensors^[60,61] or, most interestingly, as force probes, either at the macroscale^[52,53,62] or at the micro- or nanoscale.^[42,51,63,64] Inspired by the several advantages of PDAs, we implemented the mechanofluorochromism in devices applied to bioscience: thanks to the marriage between the new advanced fluorescence detection techniques and the microfluidics engineering, and to the multidisciplinary cooperation between chemistry, material sciences, and biophysics, we report herewith a new procedure to embed polydiacetylenes in microfluidic devices, as well as a new method to detect the microscale friction forces exerted by *C. reinhardtii* microalgae when compressed in restricted channels.

2. Results and Discussion

2.1. Design and Synthesis

Aiming at a covalent functionalization of silane-based surfaces, such as glass and polydimethylsiloxane (PDMS), we designed a precursor (DA, Scheme 1) made of a central photopolymerizable diacetylene unit and two symmetric arms bearing one terminal triethoxysilane unit each. The choice of a symmetric structure containing urethane units is dictated by the need of

close proximity between the diacetylenic units to be prone to photopolymerization.^[36,41] The possibility of a double anchoring of the first DA layer via the triethoxysilane groups and of a self-assembly of other DA units through the urethane functions is likely to favor a rigid supramolecular arrangement fulfilling the geometrical requirements.^[36,63,64] DA was synthesized by reaction of commercial 5,7-dodecadiyne-1,12-diol and 3-(triethoxysilyl)propyl isocyanate in toluene at 60°C . The desired compound is obtained after purification in acceptable yield (39%).

2.2. Surface Functionalization and Characterization

A preliminary characterization of polydiacetylene PDA was conducted on glass surfaces, coated according to the procedure reported by Peng et al.^[65] Precursor DA (≈ 20 mg) was dissolved in isopropanol (iPrOH, 0.5 mL), then 0.3 mL of aqueous HCl (0.1 M) was added. HCl acts as a catalyst to prompt the hydrolysis of the triethoxysilane groups and increase their reactivity toward the glass surface. The solution was carefully mixed and deposited on a clean glass slide, to allow covalent reaction between the —OH groups along the surface and the terminal triethoxysilane groups. After complete evaporation of the organic solvent, the slide was washed by sonication in clean iPrOH and dried. A medium-pressure mercury lamp (254 nm) was used to induce photopolymerization of DA to the PDA phase. Throughout the photoreaction (Figure 1), UV–vis absorption spectroscopy revealed the first appearance of an absorption band centered at 604 nm, corresponding to the so-called “purple” form of PDA,^[40,41,54] and its consequent transformation toward the “red” phase, the main band moving toward shorter wavelengths (see Figure S4, Supporting Information for details). As previously reported,^[56,66,67] prolonged light irradiation can lead to a partial conversion to the red phase, thus, in all the experiments carried out thereafter, the irradiation time was kept short or the light intensity low. The resulting purple phase emits in the red region, with a low-intensity broad band centered at 700 nm. Moreover, as in the case of similar compounds,^[41,42,46,54] the purple phase is in thermal equilibrium with the blue one, but their reversible interconversion occurs fast and at low temperature (below 0°C), thus the characterization of the blue PDA, which is beyond the scope of this work, will not be reported hereby.

The general morphology of the PDA phase, investigated by means of optical microscopy, consists of a layer of droplet-like aggregates, whose diameters range from tens to hundreds of micrometres, even though a larger extent and homogeneity of coverage can be obtained by increasing the concentration of the precursor solution. The particles formation is ascribable to two main processes occurring as the solvent evaporates, that is, a partial precipitation of DA and the self-reaction of the hydrolyzed silane groups. Hence, as soon as a solid particle is

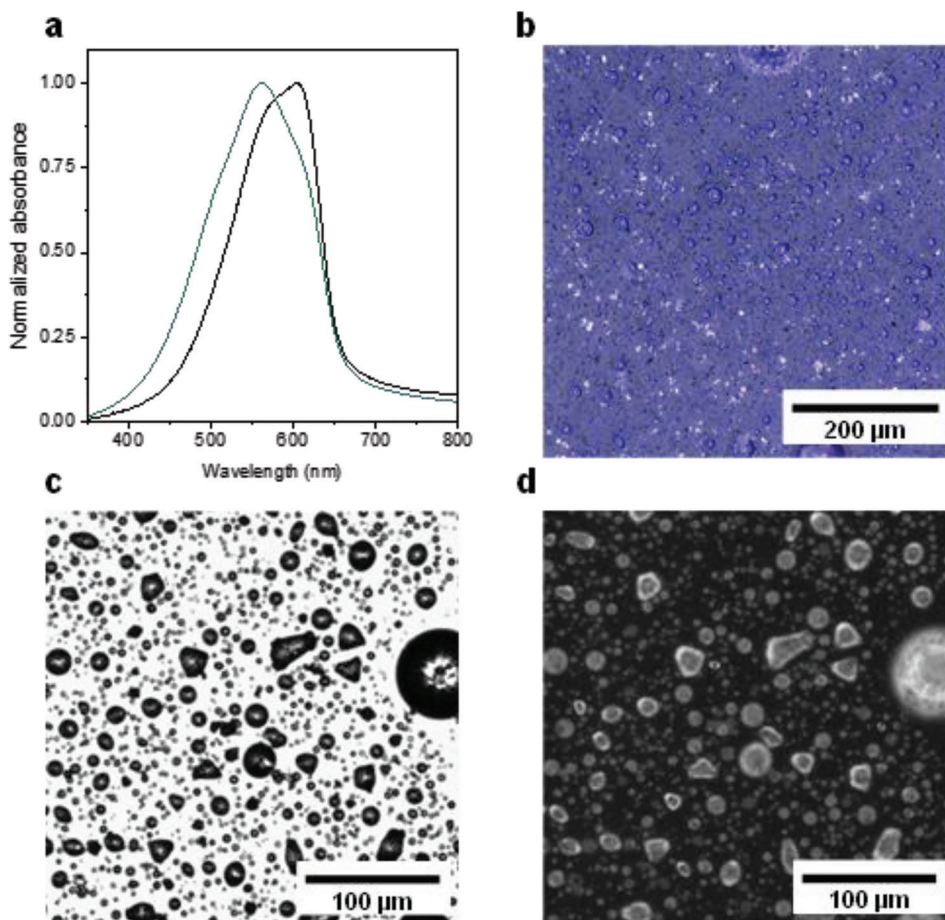


Figure 1. a) absorption spectra of PDA at low irradiation times (30 s at 2.3×10^{-8} Einstein s^{-1} , 254 nm, black full line) and at high irradiation times (45.5 min at 2.3×10^{-8} Einstein s^{-1} , 254 nm, green full line); b–d) microscopy of PDA deposited on glass slides in b) reflectance, c) transmission, and d) fluorescence mode ($\lambda_{exc} = 488$ nm).

formed, it can undergo ambient light photopolymerization with neighbouring molecules prior to its grafting onto the glass surface, which is likely to occur on longer timescales. Nevertheless, the degree of covalent grafting between the triethoxysilane groups and the glass surface resulted to be efficient, as, after careful rinsing, only a minor portion of unreacted material was removed.

Upon excitation at 488 nm, the PDA displays a low red fluorescence, while the boundaries of the particles and of the functionalized areas emit in the green region (Figure 2c). Such a discrepancy can be explained on account of the particles shape. The center of the particle is thicker, thus light cannot easily penetrate completely down to the PDA-glass interface and more time is required to achieve the same degree of photopolymerization. In contrast, the photopolymerization at the borders is more pronounced, leading first to the purple form, easily followed by a quick partial conversion to the red form, which emits in the green region (vide infra). It must be underlined that the red form being more intensely emitting (vide infra) than the purple one, even a minor percentage of its green emission can overcome the low red emission of the purple form.

2.3. Mechanoresponsivity

The PDA-coated glass surfaces proved to be mechanochromic and mechanofluorochromic upon a shearing stress. When the material is scratched with a stiff metal needle, most of the material is removed and no color or emission can be appreciated. Instead, when the surface is scratched with a softer cotton stick, the color gradually changes from purple to red, with an intensity qualitatively increasing with the force manually applied on the surface (Figure 2a). Once converted to the red form, no backward process is observed, even after several months, therefore the mechano-induced transition from the purple phase to the red one can be considered irreversible, in line with previous studies.^[33,41,42,45,54,55] We probed the fluorescence of the pristine and of the scratched zones by means of an optical fiber that records the emission signal on the surface of non-transparent samples. As shown in Figure 2b, the scratched zone emits with a broad band centered at 550 nm – more intense and blueshifted of ≈ 150 nm with respect to the purple form. Despite the intensity comparison between pristine and scratched form cannot be fully quantitative – due to the inhomogeneous coating and

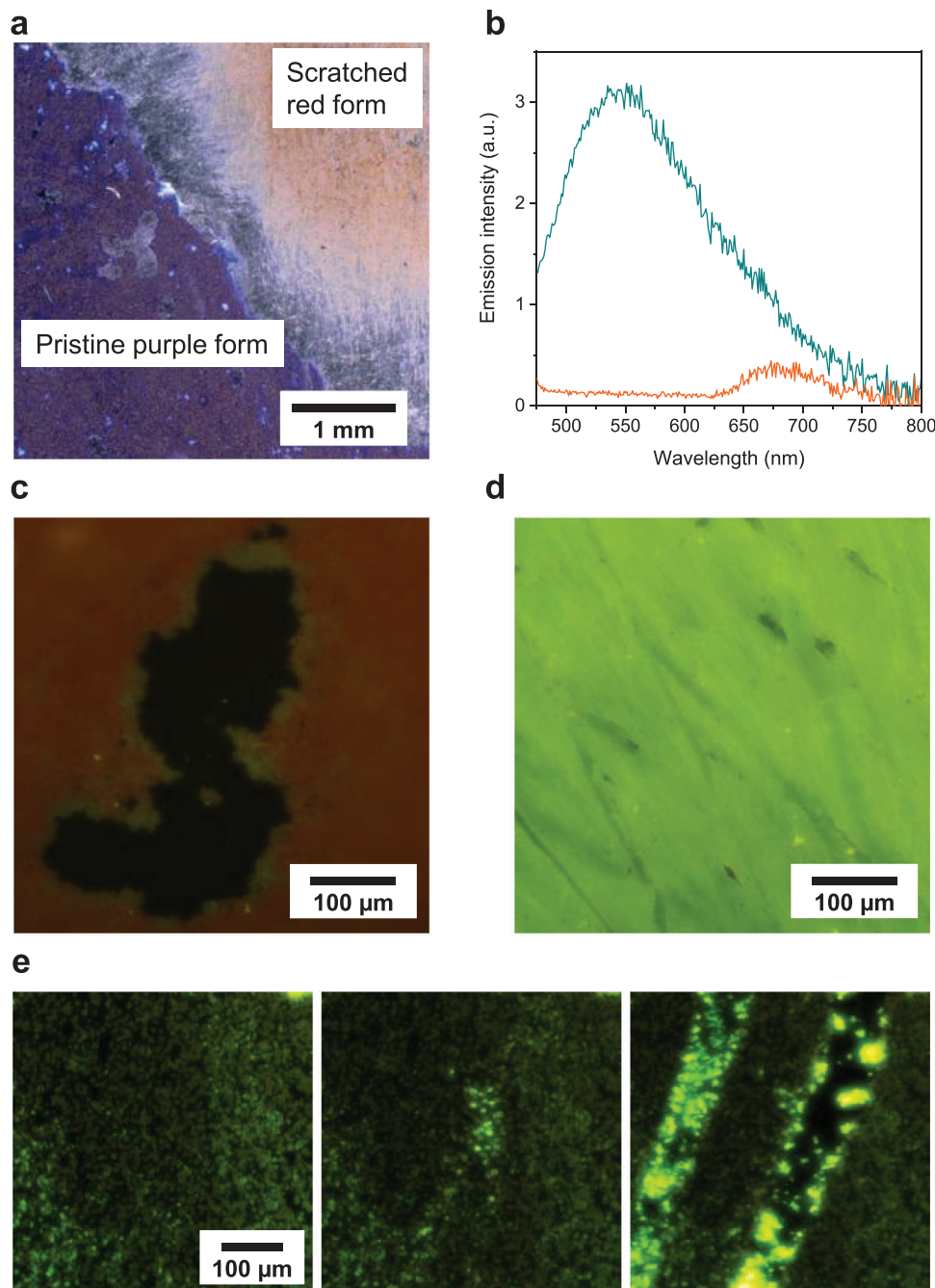


Figure 2. a) optical microscopy of PDA on a glass slide, in its pristine form (bottom left) and scratched form (top right); b) emission spectra of the pristine (orange line) and scratched (green line) forms; c) emission microscopy ($\lambda_{\text{exc}} = 488 \text{ nm}$) of the pristine purple form (exposure time 500 ms); the dark area at the center is a non-functionalized zone; d) emission microscopy ($\lambda_{\text{exc}} = 488 \text{ nm}$) of the scratched red form (exposure time 100 ms); e) emission microscopy after consecutive scratches on the surface a glass slide, recorded from the bottom of the glass slide (exposure time 500 ms, extracted from Video S1, Supporting Information); the more intense areas correspond to the mechanical solicitations.

thickness of the sample – we observed a larger emission intensity in the green phase, as reported in Figure 2c,d. As mentioned above, samples obtained by deposition of a low-concentration solution of DA give particle-like coatings, where the particles borders emit green light, most likely due to a minor contribution of the highly emitting red phase. Indeed, upon scratching the

surface of a PDA-coated glass slide with the tip of a metallic needle, and recording the fluorescence with a microscopy setup from the bottom of the sample, a marked enhancement of the green emission is observed, proving that most of the deposited material turns to the red, green-emitting phase (Figure 2e; Video S1, Supporting Information).

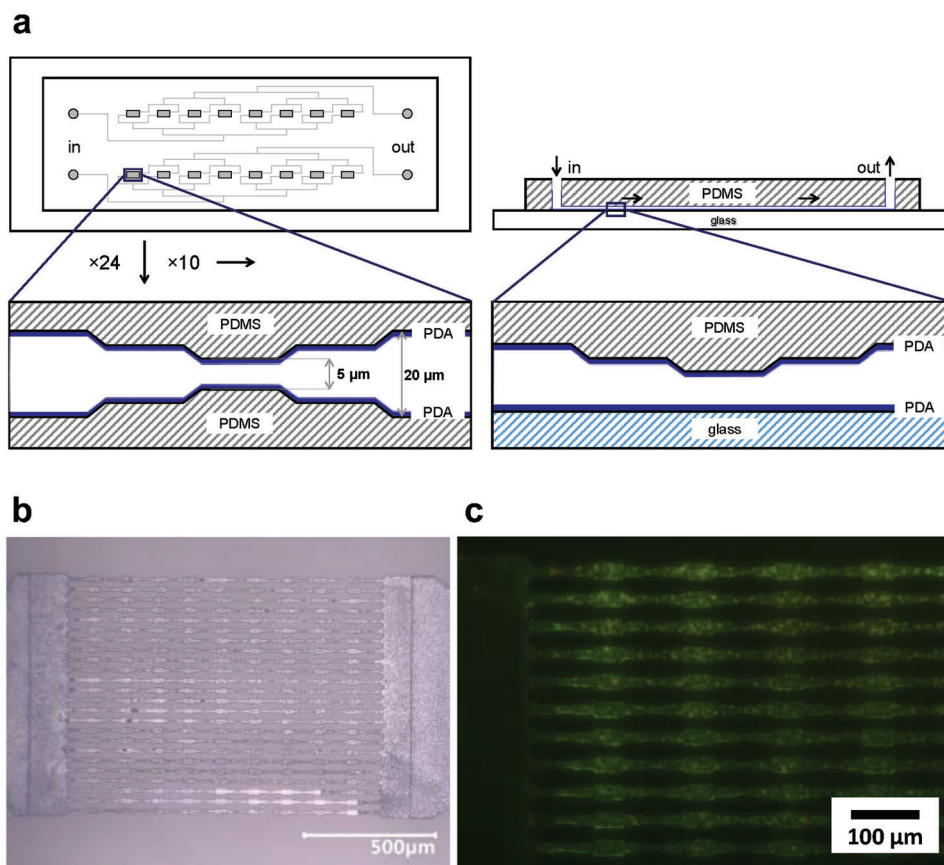


Figure 3. a) top view (left) and side view (right) schematic representation of the microfluidic chips; b) numerical optical and c) epifluorescence ($\lambda_{\text{exc}} = 488 \text{ nm}$ – background signal is subtracted) microscopy images of the PDA-functionalized channels.

2.4. Microfluidic Chips Functionalization

Compression experiments on microalgae were performed on previously reported microfluidic devices,^[17,18] specifically designed to exert a cyclic compressive stress (**Figure 3a**). The flow is spread and forced into eight analysis frames, each containing 24 compressive channels. Each channel is composed of 10 consecutive restrictions having a size ($5 \mu\text{m} \times 5 \mu\text{m}$) smaller than the cell diameter (usually $>10 \mu\text{m}$). Microchips were functionalized with a similar procedure as for glass slides. A solution of **DA** was poured into the chip from the inlet, by means of a glass pipette, until complete filling of the channels. The solution was let react for $\approx 30 \text{ min}$, to allow covalent grafting of the PDA with the surrounding groups of the microchannels, then the chip was purged with air and exposed to low-intensity UV light for 10 min. Prior to the use with biological samples, the chip was further washed with pure water to remove any unbound PDA particle. The morphology of PDA in the functionalized channels (**Figure 3b,c**) is similar to that observed on glass supports: the **DA** precursor deposits and binds to glass and PDMS in small aggregates. However, particles with a diameter larger than the channel lumen that form during the **DA** deposition can clog part of the channel and prevent from a complete functionalization. The fluorescence signal is maintained in the channels, and the particles display a low red emission in the center and a brighter green emission on the

borders. Instead, in the unfunctionalized clogged channels no emission is observed, ruling out a possible self-fluorescence of the PDMS matrix. The fluorescence signal is not affected by the flow of water or other liquid media: no appreciable emission variation is observed, as well as no PDA removal. In contrast, prolonged exposure to the epifluorescence excitation light at 488 nm caused a noticeable photobleaching^[68] of the PDA (see **Figure S5**, Supporting Information) and led to a non-negligible disappearance of the fluorescence signal.

2.5. Force Detection in Microfluidics

The possibility of detecting the stress exerted by compression of cells was proven employing *C. reinhardtii* microalgae, which are well known to possess a cellular envelope with a suitable rigidity to friction onto the PDA coating in the channel restrictions.^[18,19,69] The cells were cultured in tris-acetate-phosphate (TAP) medium. At the moment of the experiment, the microalgae possess an average diameter of 15 μm . The microalgal solution was forced into the microfluidic chip at the pressure of 700 mbar. The flow was monitored under an optical microscope, in epifluorescence mode, exciting at 488 nm, and collecting the emission through a 500 nm long-pass filter by a CCD camera. The output in true colors obtained with this setup

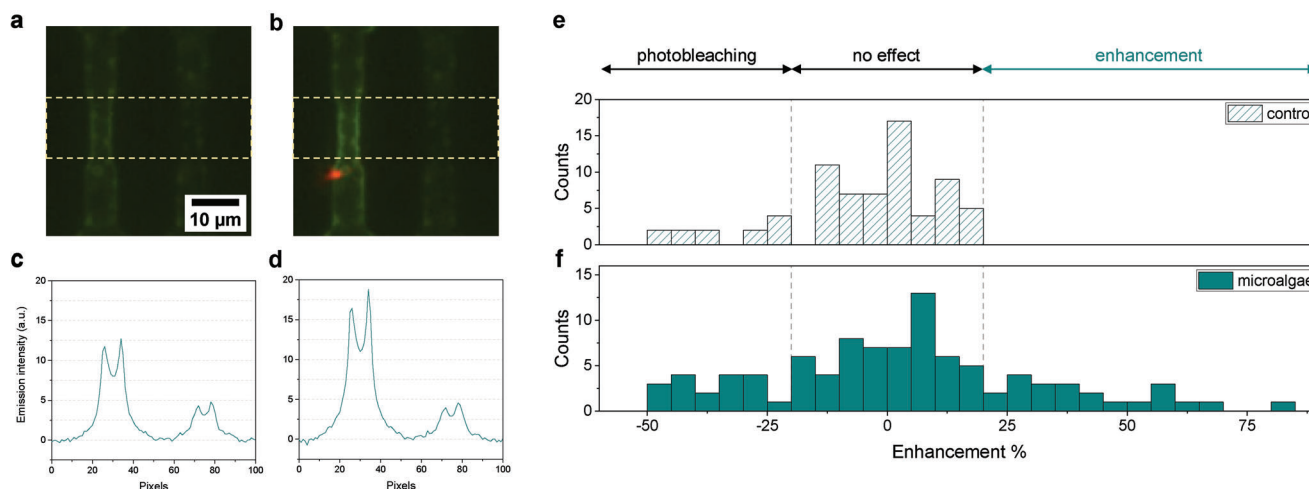


Figure 4. a,b) epifluorescence images of two restrictions before (a, time 00:25 in Video S2, Supporting Information) and after (b, time 00:50 in Video S2, Supporting Information) algae flow; c,d) intensity profiles of the region of interest (dashed yellow line in (a,b), matrix 32×100 pixels) c) before and d) after algae flow; a microalga is visible as a bright red spot in (b); e) histograms of fluorescence enhancement of the control and f) of the restrictions containing microalgae.

allows to discriminate between PDA, appearing as bright green or low-intensity red small spots, which do not move during the experiment, as they are covalently bound to the substrates, and the microalgae, which appear as round spots brightly emitting in the red, due to the chlorophylls, and moving with the flow (Figure 4b). The real-time monitoring of the algae passage can be visualized in Video S2 (Supporting Information). We found out that in clogged channels only the medium was able to flow, whereas cells remained blocked before the clog, confirming the efficiency and stiffness of the covalent binding. As it happened for water, the passage of the sole TAP medium did not affect the fluorescence signal, but compression of one or more cells into the channels restrictions resulted in a marked fluorescence enhancement. Figure 4a shows a selected region of interest, indicated in Video S2 (Supporting Information) by a red square and rotated clockwise of 90° in the figure for an easier visualization, comprehensive of two restrictions, after water purge and before the passage of two cell sample. After few seconds of flow (Figure 4b; Video S2, Supporting Information), in which several microalgae passed into the left channel (see Video S3, Supporting Information) but only the TAP medium passed into the right one, the emission of the left restriction displayed a marked increase, whereas that of the right channel remained unchanged. We plotted the integral of the intensity profile in a region of interest (yellow line in Figure S4, Supporting Information) of 32×100 pixels, before and after the microalgal solution flow, as shown in Figure 4c,d, setting to zero the background of the two plots, i.e., the dark zone where no emission is observed from the undervivated glass and PDMS scaffold. The section of the channels being a $5 \mu\text{m} \times 5 \mu\text{m}$ square, the profiles of the restrictions show two peaks each, arising from the cumulative emission of PDA lying on the two walls perpendicular to the focal plane, and a central emissive zone corresponding to the top PDMS and the glass bottom walls. By integrating the area underneath the peaks, we measured a 42% enhancement for the left channel, namely from $I = 155$ counts (before the microalgae passage) to $I = 220$ counts (after the microalgae passage), no emission variations for the

right channel ($I = 57$ counts before, $I = 57$ counts after) and no remarkable photobleaching within 1 min. Therefore, we confirmed that TAP, as well as pure water, does not induce any mechanical stress on the PDA and, thus, does not affect the fluorescence intensity. Contrariwise, microalgae, having a diameter larger than the restriction section, are subject to an unavoidable cellular compression and their consequent friction on the channel walls should be considered as the unique cause of the fluorescence enhancement. In order to quantify the events and the magnitude of the enhancement, we performed a statistical analysis on a sample of more than 150 restrictions, considering henceforth all the restrictions not traversed by microalgae as control experiments, and all those traversed by microalgae and freed from any biological material. Restrictions containing microalgae after the end of the flow were disregarded to avoid emission artifacts. For these measurements, in order to minimize photobleaching, the flow of microalgae was monitored in transmission mode, and epifluorescence images were recorded only soon before and soon after their passage, exposing the device to the excitation light only for few seconds. The results are gathered in the histograms in Figure 4e. As expected, in the control experiments, the distribution of events is peaked $\approx 0\%$, since no mechanically induced fluorescence variation can be possible, yet a slight increase or decrease can be observed between -20% and 20% . We consider this interval as an intrinsic error range related to signal fluctuations of the camera, to minor misalignments of the microchip on the microscopy platform, and to the mathematical errors in the peak integration procedure. In addition, negative values can be observed down to -50% , most likely due to unavoidable photobleaching (see Figure S5, Supporting Information).

In the channels traversed by microalgae, the statistical distribution in the range between -50% and $+20\%$ reflects the control experiments, and the ratio between samples displaying no effect and samples photobleached is substantially unchanged (60:12 events for the control, 56:18 for the microalgae experiment). Nevertheless, a positive fluorescence enhancement is observed only in the microalgae experiment, where 22 out of 96 the surveyed

samples showed a fluorescence enhancement, with values up to 83%. These two distributions clearly show that the emission increase is only ascribable to the friction between the microalgae and the PDA. Moreover, the emission variation is i) possibly higher than the measured value, since the photobleaching can occur in any case and lowers the apparent enhancement; ii) distributed on a large range, considering the values that fall within the 20% but cannot be distinguished because of the intrinsic error. Overall, the broad distribution of values suggests that the magnitude of the mechanically induced fluorescence enhancement can be proportional to the number of microalgae passing into the restriction and to the stress exerted on the mechanofluorochromic layer. Indeed, both the PDA particles and the microalgae have a distribution in diameter, thus large microalgae passing through restrictions endowed with large PDA particles (i.e., with a lower accessible space in the lumen of channel) would cause larger friction and fluorescence enhancement when compared to small microalgae passing on smaller PDA particles. Thus, we believe that the fluorescence response is not a mere OFF–ON logic gate that reveals if cells have passed or not, but rather a quantitative tool that can potentially correlate the fluorescence value to the number of microalgae passed and/or to their friction with the PDA.

3. Conclusion

We designed and synthesized a diacetylene compound with two triethoxysilane-terminated arms, able to covalently graft to glass or PDMS surfaces and to photopolymerize to PDA by UV light irradiation. We then investigated the morphology of PDA-coated glass surfaces by means of spectroscopy and microscopy methods. The DA precursor is deposited in particles that bind to the glass surface, and, by photopolymerization, yield the purple phase of PDA, which emits with low intensity in the red region. Mechanical shearing stress induces an irreversible transition from the purple to the red phase, the latter being red-coloured and green emitting. We therefore applied such PDA-coating protocol to microfluidic chips specifically designed to induce a compressive stress on microorganisms flowing through restrictive channels. Following a similar procedure as for glass functionalization, we successfully coated the lumina of the microfluidic channels with PDA particles. We then applied these microfluidic devices to compress *C. reinhardtii* microalgae, which are known to have a rigid cellular envelope and are likely to undergo a compression stress when forced into the restrictions of the channels. Indeed, in clogged channels, where only the medium was able to pass, we did not notice any appreciable green fluorescence enhancement, but only fluctuations $\approx 0\%$, or rather fluorescence quenching due to photobleaching. Contrariwise, in the channels where microalgae were compressed, we measured a strong fluorescence enhancement, up to 83%. This result can only be ascribable to the friction exerted by microalgae onto the PDA-coated channel walls and uncontroversially proves the ability of PDA to detect microscale forces in microfluidic environments. In conclusion, this protocol of implementation of mechanofluorochromes in microfluidics can be further extended to other devices and paves the way to the fluorescence-based force detection not only in the field of microalgae technology but also as a diag-

nostic tool for other stress-sensitive cell types, such as cancer or blood cells.

Supporting Information

Supporting Information is available from the Wiley Online Library or from the author.

Acknowledgements

The authors acknowledge Arnaud Brosseau, Thomas Recouly, and Sébastien Paloc for their help in the experimental setups. This work was funded by the European Research Council (ERC) under the European Union's Horizon 2020 research and innovation program (grant agreement No 715757 MECHANO-FLUO) and the AAP IDA 2021 project « MecaFluoAlgues » (Institut d'Alembert, CNRS, ENS Paris-Saclay, Université Paris-Saclay).

Conflict of Interest

The authors declare no conflict of interest.

Data Availability Statement

The data that support the findings of this study are available from the corresponding author upon reasonable request.

Keywords

force probes, mechanofluorochromism, microalgae, microfluidics, polydiacetylenes

Received: April 19, 2023

Revised: June 27, 2023

Published online:

- [1] S. Behera, R. Singh, R. Arora, N. K. Sharma, M. Shukla, S. Kumar, *Front. Bioeng. Biotechnol.* **2015**, *2*, 90.
- [2] Y.-J. Juang, J.-S. Chang, *Biotechnol. J.* **2016**, *11*, 327.
- [3] T. Takeshita, *Appl. Energy* **2011**, *88*, 3481.
- [4] J. Kim, G. Yoo, H. Lee, J. Lim, K. Kim, C. W. Kim, M. S. Park, J.-W. Yang, *Biotechnol. Adv.* **2013**, *31*, 862.
- [5] M. Vanthoor-Koopmans, R. H. Wijffels, M. J. Barbosa, M. H. M. Eppink, *Bioresour. Technol.* **2013**, *135*, 142.
- [6] P. M. Slegers, B. J. Koetzier, F. Fasaie, R. H. Wijffels, G. van Straten, A. J. B. van Boxtel, *Algal Res.* **2014**, *5*, 140.
- [7] K. Miazek, L. Kratky, R. Sulc, T. Jirout, M. Aguedo, A. Richel, D. Goffin, *Int. J. Mol. Sci.* **2017**, *18*, 1429.
- [8] E. Günerken, E. D'Hondt, M. H. M. Eppink, L. Garcia-Gonzalez, K. Elst, R. H. Wijffels, *Biotechnol. Adv.* **2015**, *33*, 243.
- [9] P. R. Postma, T. L. Miron, G. Olivieri, M. J. Barbosa, R. H. Wijffels, M. H. M. Eppink, *Bioresour. Technol.* **2015**, *184*, 297.
- [10] G. S. Araujo, L. J. B. L. Matos, J. O. Fernandes, S. J. M. Cartaxo, L. R. B. Gonçalves, F. A. N. Fernandes, W. R. L. Farias, *Ultrason. Sonochem.* **2013**, *20*, 95.
- [11] A. Santana, S. Jesus, M. A. Larrayoz, R. M. Filho, *Procedia Eng.* **2012**, *42*, 1755.

- [12] R. R. Kumar, P. H. Rao, M. Arumugam, *Front. Energy Res.* **2015**, *2*, 61.
- [13] M. Goettel, C. Eing, C. Gusbeth, R. Straessner, W. Frey, *Algal Res.* **2013**, *2*, 401.
- [14] Y. S. Lai, P. Parameswaran, A. Li, M. Baez, B. E. Rittmann, *Bioresour. Technol.* **2014**, *173*, 457.
- [15] M. D. A. Zbinden, B. S. M. Sturm, R. D. Nord, W. J. Carey, D. Moore, H. Shinogle, S. M. Stagg-Williams, *Biotechnol. Bioeng.* **2013**, *110*, 1605.
- [16] A. K. Minhas, P. Hodgson, C. J. Barrow, A. Adholeya, *Front. Microbiol.* **2016**, *7*, 546.
- [17] S. Bensalem, F. Lopes, P. Bodénès, D. Pareau, O. Français, B. Le Pioufle, *Bioresour. Technol.* **2018**, *257*, 129.
- [18] P. Bodénès, F. Lopes, D. Pareau, O. Français, B. L. Pioufle, *Algal Res.* **2016**, *16*, 357.
- [19] S. Bensalem, D. Pareau, B. Cinquin, O. Français, B. Le Pioufle, F. Lopes, *Sci. Rep.* **2020**, *10*, 2668.
- [20] Y. Sagara, S. Yamane, M. Mitani, C. Weder, T. Kato, *Adv. Mater.* **2016**, *28*, 1073.
- [21] K. Ariga, T. Mori, J. P. Hill, *Adv. Mater.* **2012**, *24*, 158.
- [22] P. Xue, J. Ding, P. Wang, R. Lu, *J. Mater. Chem. C* **2016**, *4*, 6688.
- [23] M. M. Caruso, D. A. Davis, Q. Shen, S. A. Odom, N. R. Sottos, S. R. White, J. S. Moore, *Chem. Rev.* **2009**, *109*, 5755.
- [24] Y. Sagara, T. Kato, *Nat. Chem.* **2009**, *1*, 605.
- [25] D. A. Davis, A. Hamilton, J. Yang, L. D. Cremer, D. Van Gough, S. L. Potisek, M. T. Ong, P. V. Braun, T. J. Martínez, S. R. White, J. S. Moore, N. R. Sottos, *Nature* **2009**, *459*, 68.
- [26] J. Kunzleman, M. Gupta, B. R. Crenshaw, D. A. Schiraldi, C. Weder, *Macromol. Mater. Eng.* **2009**, *294*, 244.
- [27] C. Calvino, E. Henriët, L. F. Muff, S. Schrettl, C. Weder, *Macromol. Rapid Commun.* **2020**, *41*, 1900654.
- [28] H. Müller, C. J. Eckhardt, *Mol. Cryst. Liq. Cryst.* **1978**, *45*, 313.
- [29] D. Yan, D. G. Evans, *Mater. Horiz.* **2014**, *1*, 46.
- [30] C. Calvino, A. Guha, C. Weder, S. Schrettl, *Adv. Mater.* **2018**, *30*, 1704603.
- [31] L. Ma, X. Feng, S. Wang, B. Wang, *Mater. Chem. Front.* **2017**, *1*, 2474.
- [32] X. Sun, T. Chen, S. Huang, L. Li, H. Peng, *Chem. Soc. Rev.* **2010**, *39*, 4244.
- [33] R. W. Carpick, D. Y. Sasaki, M. S. Marcus, M. A. Eriksson, A. R. Burns, *J. Phys. Condens. Matter* **2004**, *16*, R679.
- [34] S. Okada, S. Peng, W. Spevak, D. Charych, *Acc. Chem. Res.* **1998**, *31*, 229.
- [35] A. Sarkar, S. Okada, H. Matsuzawa, H. Matsuda, H. Nakanishi, *J. Mater. Chem.* **2000**, *10*, 819.
- [36] D.-C. Lee, S. K. Sahoo, A. L. Cholli, D. J. Sandman, *Macromolecules* **2002**, *35*, 4347.
- [37] G. Chen, Y. Cui, X. Chen, *Chem. Soc. Rev.* **2019**, *48*, 1434.
- [38] X. Qian, B. Städler, *Chem. Mater.* **2019**, *31*, 1196.
- [39] R. A. Nallicheri, M. F. Rubner, *Macromolecules* **1991**, *24*, 517.
- [40] M. Schott, *J. Phys. Chem. B* **2006**, *110*, 15864.
- [41] J.-S. Filhol, J. Deschamps, S. G. Dutremez, B. Boury, T. Barisien, L. Legrand, M. Schott, *J. Am. Chem. Soc.* **2009**, *131*, 6976.
- [42] R. W. Carpick, D. Y. Sasaki, A. R. Burns, *Langmuir* **2000**, *16*, 1270.
- [43] O. Yarimaga, J. Jaworski, B. Yoon, J.-M. Kim, *Chem. Commun.* **2012**, *48*, 2469.
- [44] Y. Tomioka, N. Tanaka, S. Imazeki, *J. Chem. Phys.* **1989**, *91*, 5694.
- [45] Y. Lifshitz, A. Upcher, O. Shusterman, B. Horovitz, A. Berman, Y. Golan, *Phys. Chem. Chem. Phys.* **2010**, *12*, 713.
- [46] Y. Lifshitz, A. Upcher, A. Kovalev, D. Wainstein, A. Rashkovsky, L. Zeiri, Y. Golan, A. Berman, *Soft Matter* **2011**, *7*, 9069.
- [47] K. Kuriyama, H. Kikuchi, T. Kajiyama, *Langmuir* **1998**, *14*, 1130.
- [48] A. C. S. Pires, N. d. F. F. Soares, L. H. M. Da Silva, M. C. H. Da Silva, A. B. Mageste, R. F. Soares, Á. V. N. C. Teixeira, N. J. Andrade, *J. Phys. Chem. B* **2010**, *114*, 13365.
- [49] R. R. Chance, *Macromolecules* **1980**, *13*, 396.
- [50] D. H. Charych, J. O. Nagy, W. Spevak, M. D. Bednarski, *Science* **1993**, *261*, 585.
- [51] H. Feng, J. Lu, J. Li, F. Tsow, E. Forzani, N. Tao, *Adv. Mater.* **2013**, *25*, 1729.
- [52] H. Terada, H. Imai, Y. Oaki, *Adv. Mater.* **2018**, *30*, 1801121.
- [53] J. P. Lee, H. Hwang, S. Chae, J.-M. Kim, *Chem. Commun.* **2019**, *55*, 9395.
- [54] A. A. Deckert, J. C. Horne, B. Valentine, L. Kiernan, L. Fallon, *Langmuir* **1995**, *11*, 643.
- [55] C. Phollookin, S. Wacharasindhu, A. Ajavakom, G. Tumcharern, S. Ampornpun, T. Eaidkong, M. Sukwattanasinitt, *Macromolecules* **2010**, *43*, 7540.
- [56] J. Song, J. S. Cisar, C. R. Bertozzi, *J. Am. Chem. Soc.* **2004**, *126*, 8459.
- [57] J.-M. Kim, Y. B. Lee, D. H. Yang, J.-S. Lee, G. S. Lee, D. J. Ahn, *J. Am. Chem. Soc.* **2005**, *127*, 17580.
- [58] D. J. Ahn, J.-M. Kim, *Acc. Chem. Res.* **2008**, *41*, 805.
- [59] S. Lee, J.-Y. Kim, X. Chen, J. Yoon, *Chem. Commun.* **2016**, *52*, 9178.
- [60] M. A. Reppy, B. A. Pindzola, *Chem. Commun.* **2007**, *42*, 4317.
- [61] X. Chen, G. Zhou, X. Peng, J. Yoon, *Chem. Soc. Rev.* **2012**, *41*, 4610.
- [62] S. Chae, J. P. Lee, J.-M. Kim, *Adv. Funct. Mater.* **2016**, *26*, 1769.
- [63] L. Polacchi, A. Brosseau, R. Métivier, C. Allain, *Chem. Commun.* **2019**, *55*, 14566.
- [64] L. Polacchi, A. Brosseau, R. Guillot, R. Métivier, C. Allain, *Phys. Chem. Chem. Phys.* **2021**, *23*, 25188.
- [65] H. Peng, J. Tang, J. Pang, D. Chen, L. Yang, H. S. Ashbaugh, C. J. Brinker, Z. Yang, Y. Lu, *J. Am. Chem. Soc.* **2005**, *127*, 12782.
- [66] Q. Huo, K. C. Russell, R. M. Leblanc, *Langmuir* **1999**, *15*, 3972.
- [67] A. Pankaew, N. Traiphol, R. Traiphol, *Colloids Surf., A* **2021**, *608*, 125626.
- [68] D. Bloor, M. R. Worboy, *J. Mater. Chem.* **1998**, *8*, 903.
- [69] S. K. Min, G. H. Yoon, J. H. Joo, S. J. Sim, H. S. Shin, *Sci. Rep.* **2014**, *4*, 4675.